Custom-Tailored Cross-Cylinder Tribotest to Emulate Wear Mechanism in Drilling of CFRP-Ti Stacks

Sharjeel Ahmed Khan, Nazanin Emami, Amilcar Ramalho

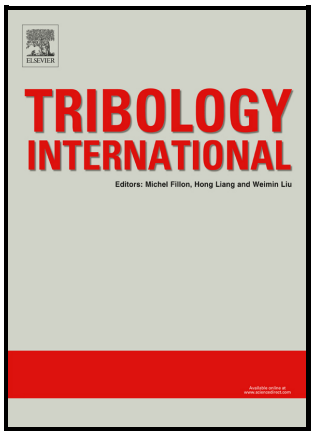

PII: S0301-679X(23)00376-6

DOI: https://doi.org/10.1016/j.triboint.2023.108589

Reference: JTRI108589

To appear in: *Tribology International*

Received date: 4 January 2023
Revised date: 3 May 2023
Accepted date: 8 May 2023

Please cite this article as: Sharjeel Ahmed Khan, Nazanin Emami and Amilcar Ramalho, Custom-Tailored Cross-Cylinder Tribotest to Emulate Wear Mechanism in Drilling of CFRP-Ti Stacks, *Tribology International,* (2023) doi:https://doi.org/10.1016/j.triboint.2023.108589

Custom-Tailored Cross-Cylinder Tribotest to Emulate Wear Mechanism in Drilling of CFRP-Ti Stacks

Sharjeel Ahmed Khan [1,2*], Nazanin Emami [2], Amilcar Ramalho [1*]

[1]Department of Mechanical Engineering, CEMMPRE, ARISE, University of Coimbra, Rua Luis Reis Santos, 3030-788, Coimbra, Portugal

[2]Department of Engineering Sciences and Mathematics, Division of Machine Element, Luleå University of Technology, 97187 Luleå, Sweden

Correspondence: * sharjeel.ahmed.khan@ltu.se ; amilcar.ramalho@dem.uc.pt

Abstract

While drilling of CFRP-Ti stacks, tool experiences complex tribomechanical interaction due to dissimilar workpiece constituents. For emulating tool wear behaviour, the typical tribotest configuration such as reciprocating and pin-on-disc test are not representative for imitating contact scenario underwent during the drilling operation. Cross-cylinder tribotest is an effective test configuration to emulate contact in different manufacturing processes by providing fresh contact surface during sliding. In this work, for the first-time, tool wear of WC-Co cylinders was analysed in cross-cylinder configuration against multi-material stack arrangement. Moreover, cross-cylinder testing against multi-material $[CFRP\text{-}Ti]_n$ workpiece showed cyclic variation in coefficient of friction against different workpiece constituents and wear mechanism is a combination of adhesive and abrasive wear on WC-Co tool, comparable to actual drilling operation.

Keywords

Cross-cylinder tribotest; CFRP-Ti stacks; difficult-to-machine materials; wear

Introduction

With the increased demands for improved fuel efficiency and environmentally friendly alternatives, the use of light weight composite structural parts for the aerospace and aeronautic industry is growing at a rapid pace. Particularly, the use of CFRP coupled with titanium are gaining popularity due to high strength to weight ratio, high galvanic corrosion resistance and excellent load bearing capabilities, making it desirable material for new generation of modern

aircrafts [1]. In Airbus A350 and Boeing 787, CFRP-Ti stacks are employed in primary aircraft structural components like fuselage, aircraft wing spar and ribs to benefit from exceptional properties of both materials [2]. The demand for CFRP-Ti and other stacks combination is speculated to soar in near future due to growing trend toward sustainability, however inadequate machinability of such stacks could hinder their widespread usability.

Drilling of CFRP-Ti stacks is inevitable for making holes for rivets and fastener assembly. The exceptional material properties of CFRP-Ti stacks pose unmatched difficulty in its drilling and machining, knowing the fact that both CFRP and titanium alloys were classified as difficult-to-machine materials. The machining of these composite-metal stacks causes severe tool wear and cutting induced damages like interfacial delamination, poor surface finish and unacceptable quality of machine parts, because of disparate characteristic of workpiece constituents [3]. In order to improve the machinability and increase tool life, understanding the tool wear mechanism of CFRP-Ti stacks could provide important information about the selection of cutting parameters and further improvements to cutting tools. Previously, researchers have strived to evaluate the tool wear mechanism during drilling and machining of CFRP-Ti stacks [4–8]. However, in drilling experimental investigation, the fundamental mechanism is yet difficult to understand due to complex tool-chip interaction and cutting response of both materials. Xu et al. [9–11] performed orthogonal cutting operation on CFRP-Ti workpiece for inspection of the cutting mechanism in drilling of CFRP-Ti stacks, by employing a high speed camera for analysing dynamic chip formation mechanism in composite-metal stacks. The author reported that cutting sequence could have significant implication on the chip separation mechanism and tool wear. The chip adhesion on the tool rake face from the pre-cutting is responsible for increased tool vibration and chatter specially in region of stack interface. The cutting mechanism changes from brittle fracture to elastoplastic deformation mode in the transition zone as the tool moves from CFRP to titanium material.

Nevertheless, there is no simple evaluation method described earlier to analyse the wear mechanism of the uncoated or coated tools caused during drilling of multi-material stacks in a simple and controlled fashion, other than performing the actual drilling or cutting operation.

Cross-cylinder tribotest is a simple yet effective way to imitate the contact situation experienced during the drilling or machining operation by continually exposing the tool to fresh surface, while ensuring facile control of the contact parameters. In cross-cylinder tribotest (Fig. 1), a cylinder of large diameter acting as the workpiece material is set in rotation by fixing it inside the head of the lathe and guided by the live-center, whereas smaller cylinder acting as the tool slides across the big cylinder in the axial direction with a uniform feed rate. An appropriate feed rate was opted by Hertzian contact model and experimental trials to guarantee contact against fresh material surface during the test.

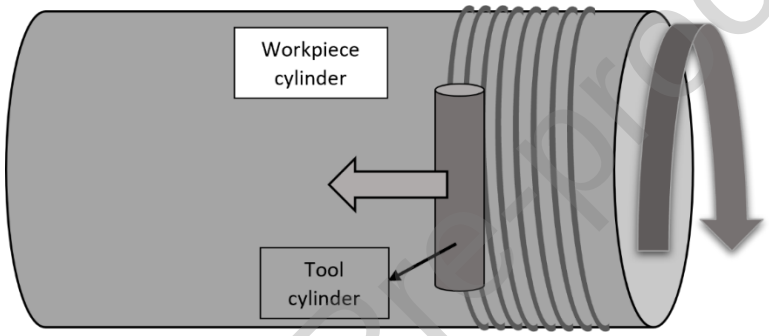

Fig. 1: Schematic of cross-cylinder tribological test

Despite the fact that cross-cylinder test was proposed in 1989 by Hedenqvist [12], it is recommended in some current studies as an optimal solution to simulate tribological contact scenarios for forming and machining operation [13,14]. Recently, the effectiveness of the cross-cylinder tribotest has been demonstrated to mimic the tool wear mechanism during turning of titanium alloy [15]. Table 1 shows a brief literature background on the cross-cylinder tribotest technique employed to mimic the tribological interaction in various manufacturing processes like rock-drilling, machining, turning, tool chip interaction, mounts in zipper industry; and the influence of different parameters on the wear behaviour of the tool was discussed. This tribotest configuration has numerous benefits like higher degree of control i.e. start/stop test on demand to evaluate wear, reduced effect of machined chips interfering with acquisition of data and flexibility to perform test for long travel distance. Moreover, test could be performed in intermittent and continuous mode to mimic tool-workpiece tribological interaction while avoiding the edge deterioration effect caused by plastic deformation or chipping.

Table 1: Cross-cylinder tribotest employed to mimic different processing applications and different parameters analysed in the literature.

Tool cylinder	Tool cylinder coatings	Workpiece cylinder	Parameters analysed	Application simulated	Ref
M2 steel PM HSS steel	uncoated TiN	AISI 1045 AISI 4340 AISI 321	Wear mechanism, friction, effect of sliding speed	Machining	[16]
HSS tool steel	TiN, CrN, TiCN, N/TiN, N/TiAlN, N/TiAlN+Al_20_3 (N/= nitrided)	Carbon steel S45C (JIS) Pure Copper	Normal load Sliding speed Counter materials Sliding distance	Forming tools	[17]
M2 steel	CN TiCN	AISI 1019 steel	Normal load Sliding speed lubricants	Metal forming tools	[13]
M2 steel Cr	W–Si–N Ck60	DIN Ck45 steel shaft	SiC abrasive particles	Miroscale abrasive wear	[18]
PM HSS steel	TiN AlCrN TiAlN Al_2O_3	20NiCrMo2 case hardening steel	Continuous and intermittent sliding mode and compared with milling insert	Milling operation	[14]
PM HSS steel HSS steel	TiN AlCrN	20NiCrMo2 case hardening steel	Surface roughness, sliding speed Continuous and intermittent sliding	Cutting tools	[19] [20]
PM HSS steel	TiN	20NiCrMo2 case hardening steel	Normal load, sliding speed, material transfer	Milling	[21]
HSS steel	TiN	Steel with 1 mass% of Si or Cr Steel with 1 mass% of Mn or Al	Effect of Si, Cr, Mn & Al in steel on material transfer and CoF	Tool-chip contact in machining	[22] [23]
WC-6%Co	-	Different rocks e.g., marble, granite etc.	Wear mechanism	Rock drilling	[24] [25]
WC-Co WC-Fe WC-Ni	-	Rock granite	Binder metal influence on WC	Rock drilling	[26]
WC-15%Co	Uncoated CrC CrN	Copper zinc alloy work hardened Oxygen free pure Copper	Wear mechanism in dry and lubricated conditions	Zipper industry	[27] [28]
WC-6%Co	-	Ti6Al4V	Wear mechanism	Turning	[15]

WC-10%Co	*-*	*Multi-material stack (CFRP-Ti) CFRP Ti*	*Sliding distance*	*Drilling & machining*	**Us*

However, to the best of our knowledge, in this work we present for the first time, a cross-cylinder tribological test employed against multi-material stack configuration with alternating arrangement of disparate material i.e., CFRP-Ti rings. In order to corroborate accuracy of the data acquisition for the lab build tribometer, the test was performed at different sliding speed against titanium to optimize the sliding parameters. Later, for one of the sliding conditions, tribotest against CFRP and CFRP-Ti stacks workpiece was performed, and wear behaviour was analysed.

Experimental

Materials

Carbon fiber reinforced polymer (CFRP) plates of 300x300x7.3mm were procured from INEGI, fabricated at 5 bar of curing pressure in an autoclave chamber using HexPly® 8552 prepreg arranged in [0°,90°] orientation, with more details given in Table 2.

Table 2: Details of CFRP workpiece

Parameter	**Specifications**
Prepreg	Hexply® 8552 UD AS4 Unidirectional fibers
Fiber orientation	$[0°,90°]_{10s}$
Fiber Filament count	12K
Fiber volume fraction	57%
Resin	Amine cured epoxy
Curing pressure	5 bar
Plate thickness	7.3mm

Moreover, Titanium Ti6Al4V alloy tubes of OD=40mm and ID=30mm was used as the workpiece material for initial testing and parameters optimization. Seamless Ti6Al4V tubes were procured from TSM Technology China, produced by deep hole drilling of extruded round bar. Table 3 shows the chemical composition of titanium tubes.

Table 3: Chemical Composition of Titanium Ti6Al4V tube

N	C	H	Fe	O	Al	V	Ti
0.05	0.08	0.015	0.4	0.2	5.5~6.75	3.5~4.5	Bal.

For the tool material, WC-Co cylinders of Ø=10mm and L=50mm were used, provided by Sandvik Coromant AB, Sweden. WC-Co cylinders has 10% of Co metal binder (H10F grade) that were polished using a metallographic sample preparation process, using 1µm diamond paste to achieve adequate surface roughness of *Ra*= 0.069±0.007 µm. The purpose of polishing is to minimize the effect of surface roughness on wear and facilitate the assessment of small changes in wear amounts against different workpiece materials. Prior to mounting the polished WC-Co cylinder in the tool holder it was cleaned with ethanol to remove any adsorbed impurities from environment.

Preparation of the workpiece shaft

Before performing the test against Ti6Al4V workpiece, the tubes were ground sequentially using SiC paper of different grits upto P2000# to alleviate the influence of surface roughness on the tribotest results. The grinding operation was repeated prior to each test and a newly ground Ti6Al4V tube was used for any subsequent trials.

Abrasive water jet machining was used for machining of CFRP plate of 7.3 mm thickness using water pressure of 5400 bar with garnet as abrasive material, at a feed rate of 385 g/min to machine rings with OD=40mm and ID=30mm from the plate (Fig. 2a). These rings were then mounted and arranged on the steel shaft with a tight dimensional tolerance to ensure a close fit. Since small dimensional variation can occur, the stack of CFRP rings were ground with SiC paper P80# and later with P120# to remove any minor variation in the rings alignment and to minimize the sudden variation in the applied load during the tribotest running. The organization of CFRP rings was specifically selected to expose the CFRP fiber acting perpendicular in contact against WC-Co to cause intense abrasive and brushing action of fibers experienced during the actual drilling operation. Following every tribotest the surface of the CFRP stacks were renewed by using an emery paper of P120# to expose the underneath surface and remove any previous surface damages from the tribotest.

To assemble shaft of multi-material stack, CFRP and Ti rings fabricated by abrasive water jet machining of plate and turning of titanium tube, respectively were employed. The titanium tubes were machined to produce rings with same thickness of 7.3mm (Fig. 2b). The rings of CFRP and Ti were then arranged in alternative fashion on a steel shaft and further secured by mechanical fastener as shown in Fig. 2c,d. The dimension of the rings were in close diameter tolerances, but in order to further ensure smooth transitions, as the tool cylinder slides across the CFRP-Ti workpiece, it was ground multiple times with SiC paper P80# and P120# to abate the effect of edge variation to the greatest extent possible. Following each tribotest, the grinding of the CFRP-Ti shaft was performed using P80# and P120# SiC paper multiple times to remove any effect from the previous testing.

Cross-cylinder tribological test

During the cross-cylinder tribotest, the tool cylinder is exposed to the fresh workpiece surface as the tool progress in the transverse direction (axial relating to the rotating shaft) with the feed rate adjusted in such a way that the tool cylinder contacts the new surface with no overlap. However, as the test progresses further a minor overlap could occur due to the wear of the tool cylinder which is quite expected. Fig. 2e shows the experimental setup employed for the tribotest. The workpiece material was held in the chuck of the lathe machine and centred by the live center. The workpiece material and tool cylinder could be easily interchanged for each test. The tool cylinder is mounted in the holder connected directly with the tangential and normal force sensor firmly held in the tool post of lathe. The tribometer was built from scratch in the lab and the components were machined separately and assembled in-house to properly hold the tool cylinder. Prior to each test, the tool cylinder was brought in close proximity of the workpiece cylinder followed by application of normal load by using dead weights, with a compliant transmission to minimize vibration. Moreover, calibration of both force sensors was performed carefully to ensure accurate data being obtained during the test. The variation in the normal and tangential forces was recorded in real time waveform spectrum from the test using Picoscope 3204A oscilloscope and Picoscope 6 software. Later the results were analysed to obtain values of CoF evolution over time/distance. Fig. 2f shows the flow chart for the data acquisition during the tribotest. A simultaneous signal generated from the tangential and normal force sensor was

amplified by an amplifier and acquired by the digital oscilloscope and then analysed to determine CoF.

Table 4 shows the test conditions employed to analyse the influence of sliding speed on the tribological properties against Ti6Al4V alloy. The test was performed at room temperature in ambient air. The CoF variation over time was analysed throughout the test. After the test, the wear tracks were analysed by SEM, EDX (Hitachi SU 3800) and 3D optical profilometry (Alicona Infinite Focus G4). Furthermore, to study the influence of workpiece cylinder i.e., multi-material stack, lowest sliding speed was selected to reduce the effect of contact temperature. The details about the test conditions and the distance travelled during the test are shown in Table 5. While sliding against CFRP-Ti workpiece, the tool cylinder is always aligned on the titanium ring and then the test was performed. After the test, the wear scar was analysed by SEM and EDX mapping to analyse the morphology and elemental composition of the transferred material respectively. Moreover, for selected sample, cross-sections were prepared by Focused Ion Beam (FIB, FEI Helios NanoLab 650) and analysed by SEM using 5KV accelerating voltage. A layer of platinum was deposited in-situ in vacuum chamber to protect the region of interest from ions during milling and polishing carried out by Gallium ions.

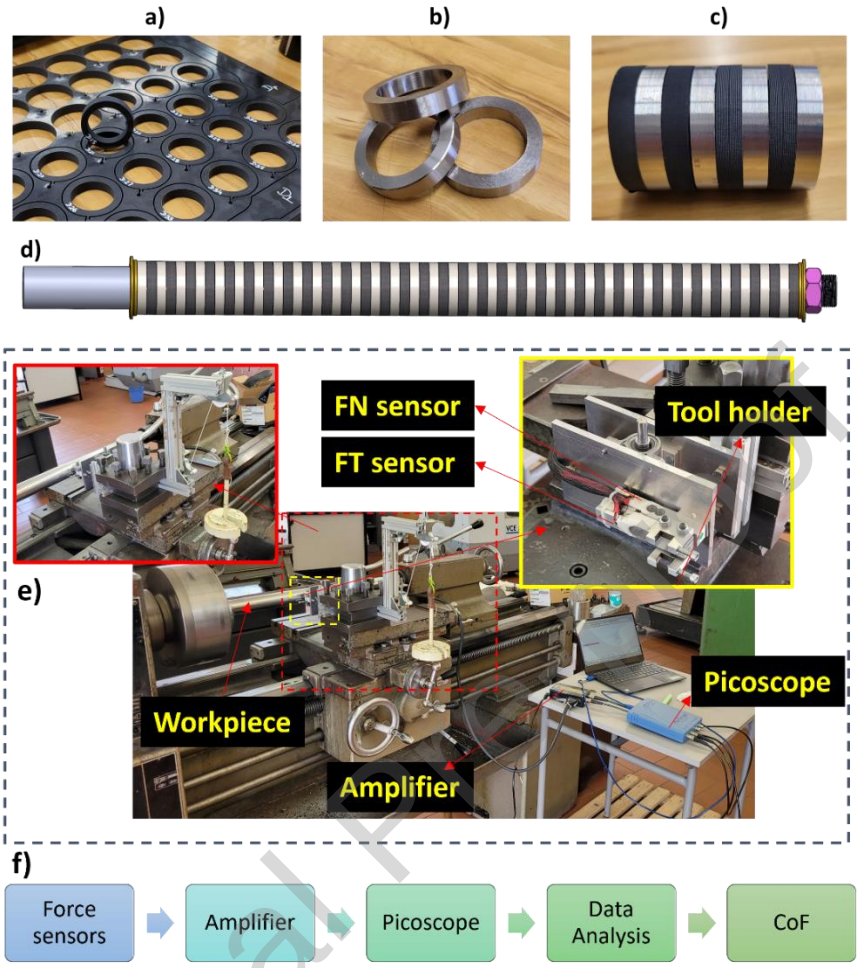

Fig. 2: a) CFRP rings machined using abrasive water jet machining b) Ti rings c) stack of CFRP and Ti rings d) schematic of assembled workpiece cylinder with alternative arrangement of CFRP (Black) and Ti (grey) rings e) Experimental configuration of triobtest f) Scheme of data acquisition from the tribotest

Table 4: Test conditions for analysing influence of different test speeds against Ti6Al4V alloy.

Parameters	**Values**			
Applied load (N)	20			
Feed rate (mm/rev)	0.3			
Outer diameter (mm)	40			
Revolution (rpm)	170	235	320	568
Sliding speed (m/min)	21.3	29.5	49.2	71.3
Total sliding distance (m)	~155	~160	~159	~154

Table 5: Sliding distance and conditions during cross-cylinder test against different workpiece materials

Parameters	Values		
Workpiece material	Ti6Al4V	CFRP	CFRP-Ti
Applied load	20 N		
Rpm	170		
Sliding speed	21.3 m/min		
Feed rate	0.3 mm/rev		
Outer diameter	40 mm		
Total sliding distance	~ 155 m	~154 m	~121 m

Results and Discussion

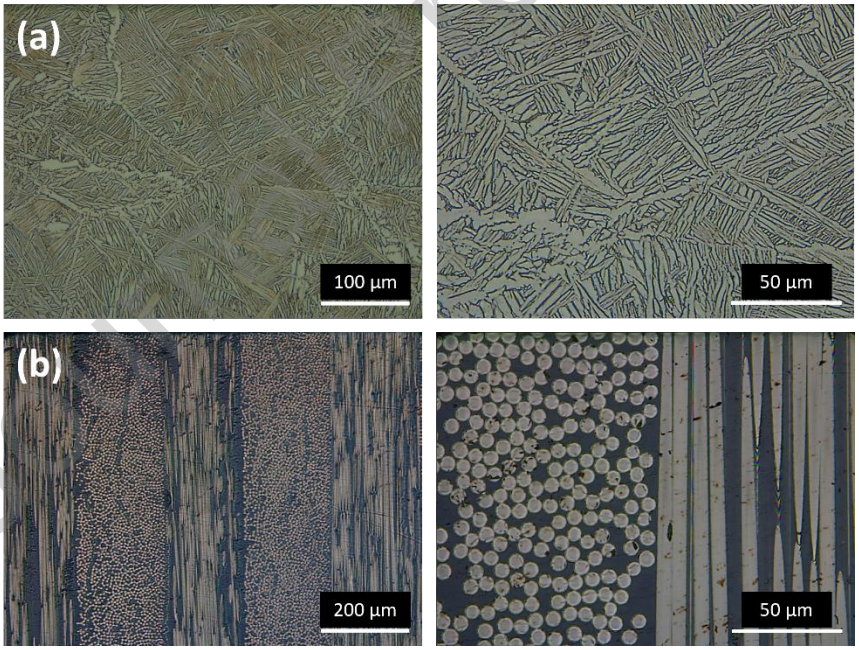

Fig. 3: Microstructure of the (a) Ti6Al4V alloy tube and (b) CFRP

Fig. 3a shows the microstructure of the cross-section of titanium (Ti6Al4V) tubes prepared by metallographic grinding, polishing route and subsequently etched with Kroll reagent (6% HNO_3 + 1%HF and 93%water). It mainly consists of two-phase lamellar microstructure in the elongated grains. The hardness of the Ti6Al4V tube was determined by applying 1kgf load using a pyramid

diamond indenter in Vickers hardness tester and it showed value of 346±13 HV_1. For the CFRP composite plate, cross-section specimen was mounted and polished by using 1µm diamond paste. The microstructure was captured by using the optical microscope showing [0°,90°] orientation of the CFRP fibers as shown in Fig. 3b. The CFRP fibers has an average diameter of 6.7±0.3µm. The predominant orientation of the fibers perpendicular to the ring contact surface would offer maximum abrasive and brushing action during the cross-cylinder testing.

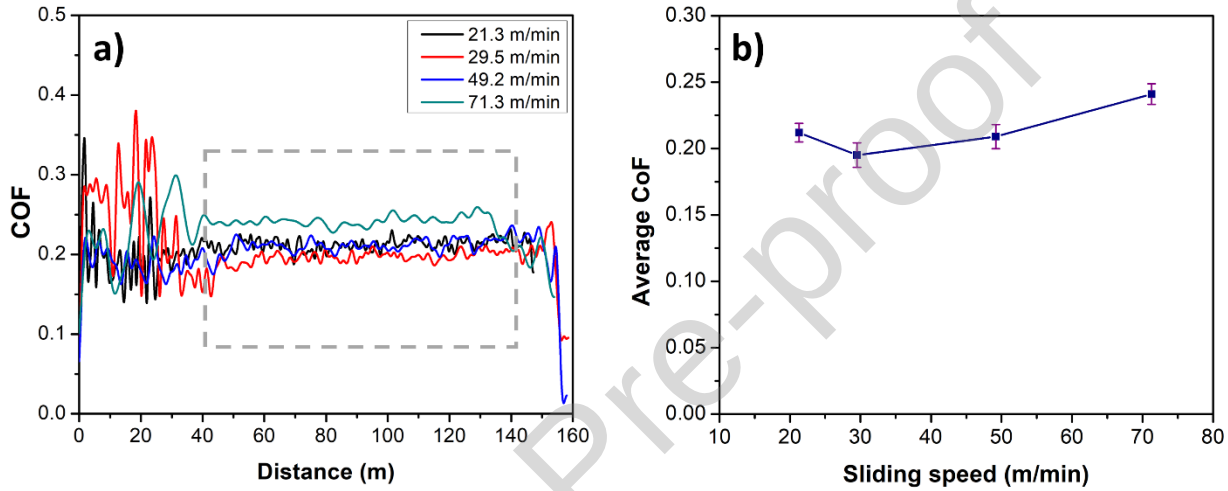

Fig. 4: a) CoF evolution with sliding distance against Ti6Al4V tube tested at different sliding speeds. b) Average CoF of the stabilized region (40-140m) as a function of sliding speed.

Fig. 4a show the evolution of CoF of WC-Co cylinder sliding against Ti6Al4V tube at different sliding speeds for a nominal sliding distance of ~157m at normal load of 20N. It was observed that CoF showed an increase in the beginning of the test associated with the running-in effect which stabilizes after 40m of travelled distance for all the sliding speeds. Fig. 4b shows the averaged CoF for the stabilized region from 40-140m of travelled distance presented as a function of the sliding speed. It showed that with an increase in the sliding speed from 21.3m/min to 29.5m/min, the average CoF decreased slightly, but with further increase in sliding speed the CoF increased gradually. In case of highest sliding speed of 71.3 m/min, the average CoF recorded was the highest that could be attributed with increased temperature and adhesive wear occurrence while sliding against reactive titanium counterbody. Despite the use of different sliding speed, the fluctuation in CoF was relatively small after the running-in period and are quite close to one another except highest sliding speed of 71.3 m/min with slightly large fluctuations.

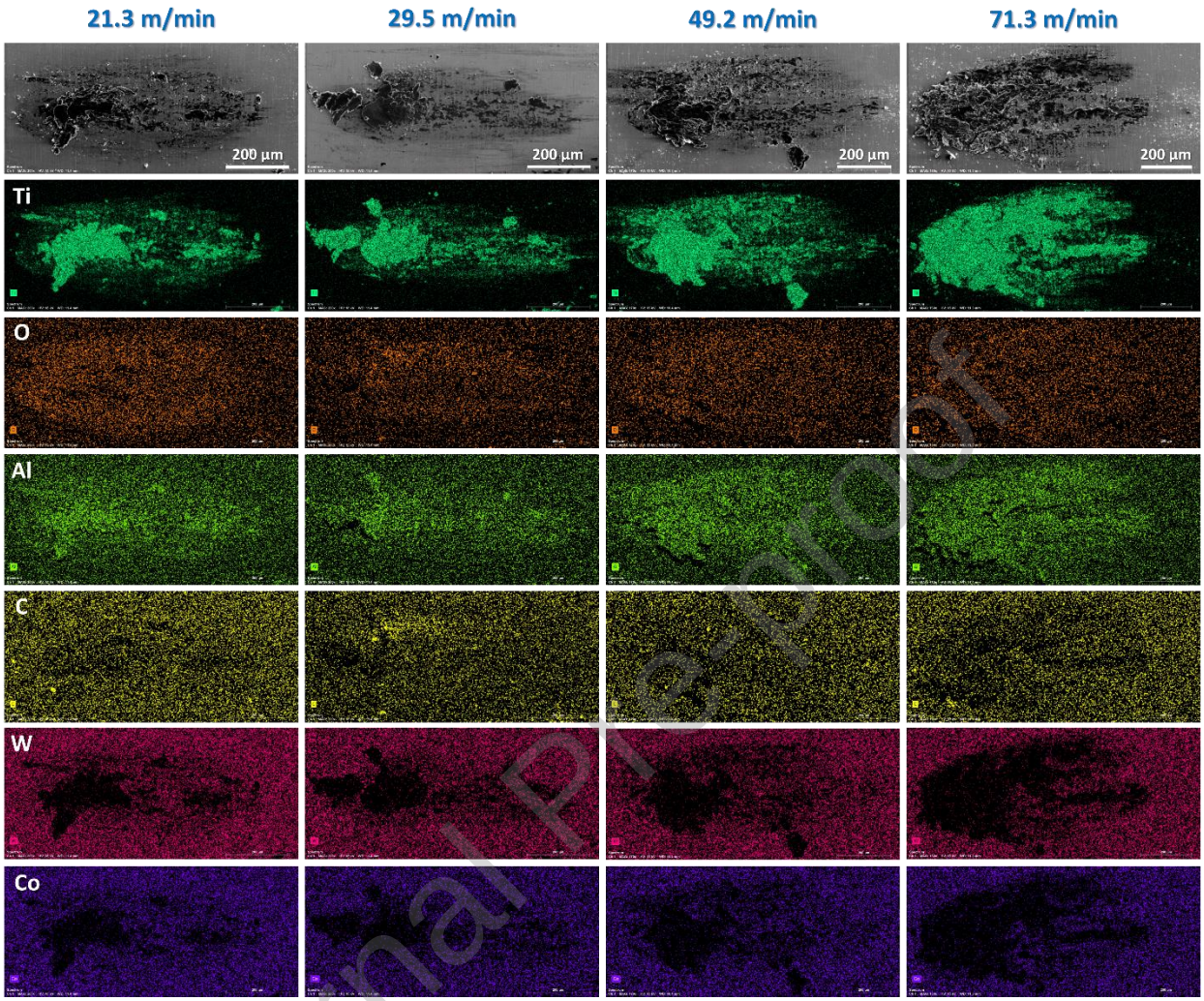

Fig. 5: EDX map of the worn region of WC-Co cylinder after sliding against Ti6Al4V tube at different sliding speed.

Fig. 5 shows the EDX map of the contact area of WC-Co cylinder tested against Ti6Al4V tube at different sliding speeds. The adhesion of the titanium increased gradually with the rise in the sliding speed. The high adhesion of titanium on the WC-Co cylinder could be the reason for the increased CoF observed during the test at higher sliding speeds. Further, the increased adhesion of aluminium in the EDX map confirms higher adhesive wear with increasing sliding speed, for both Al and Ti elemental maps, as aluminium is one of the constituents of the titanium (Ti6Al4V) alloy. Similarly, an increase in oxygen concentration was also observed with increasing sliding speed on the wear region showing oxidation. According to literature, cutting speed is one of the main factor affecting tool wear in titanium machining, and occurrence of wear phenomena like adhesion, diffusion and oxidation were accelerated between the tool-chip

interface with the increase in cutting speed [29]. The excessive adhesive wear and accumulation of titanium workpiece material dulls the cutting edge, leading in higher temperature, frictional forces and torques during the machining process [30].

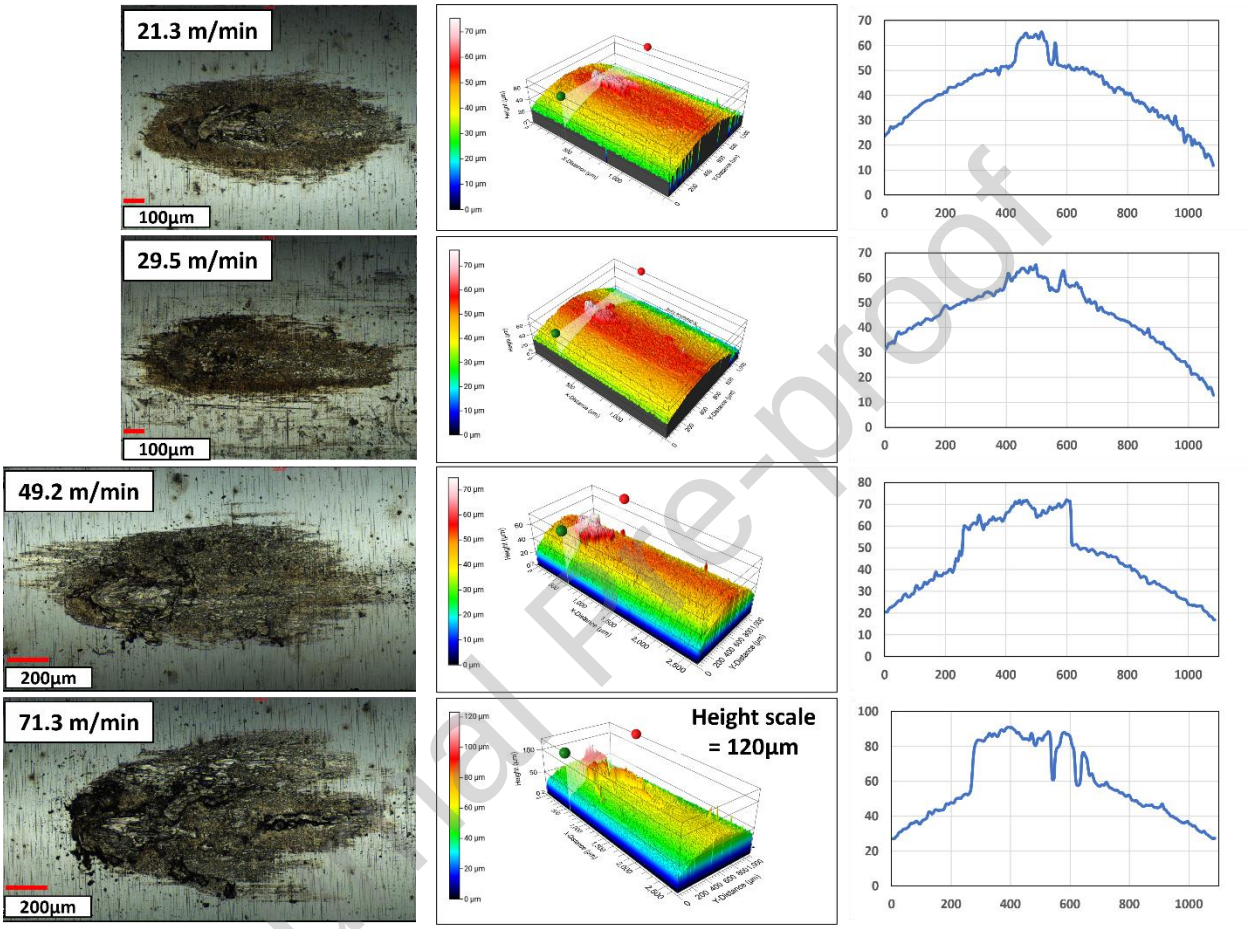

Fig. 6: 3D surface profilometry of the WC-Co cylinder sliding against Ti6Al4V at different sliding speeds and 2D surface profile of the cross-section of WC-Co cylinder.

Fig. 6 shows the 3D surface profilometry of WC-Co cylinder sliding at different sliding speed against Ti6Al4V tube. The enhanced adhesion of titanium with increasing sliding speed is clearly seen in the 2D profile of the cross-section in the worn region of the cylinder. The increased adhesion is due to highly reactive nature of titanium. A similar increase in adhesion of titanium with increasing sliding speed was also observed in the EDX maps presented earlier. Comparing the graphic on Fig. 5 with the EDX maps and the 3D profilometry results, it is possible to conclude that the evolution of the CoF with the sliding speed is governed by titanium transfer to the WC-Co countersurface.

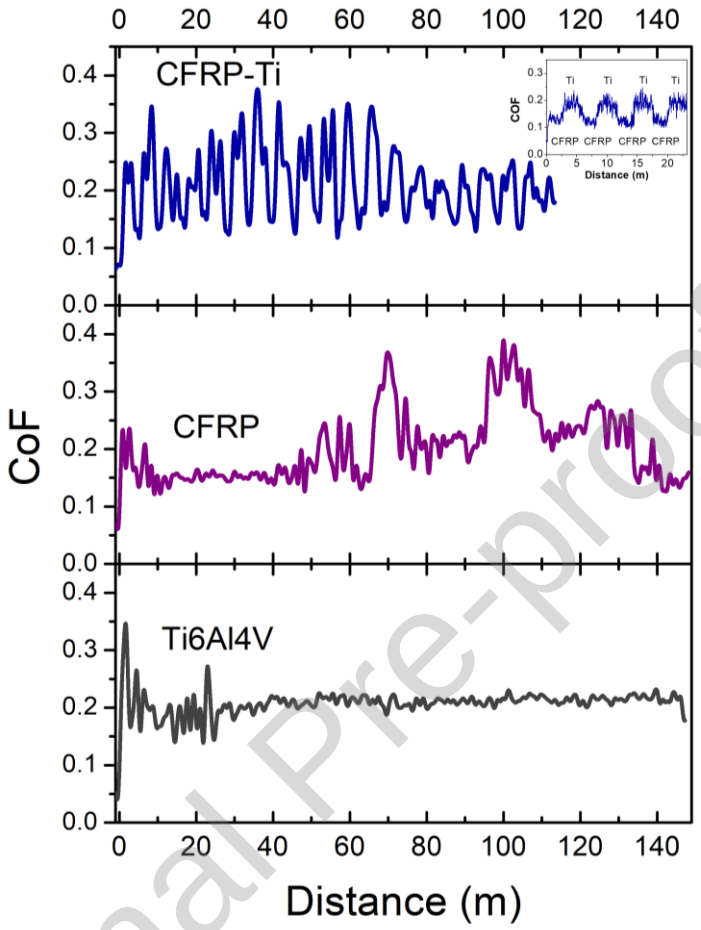

Fig. 7: CoF evolution of WC-Co cylinder sliding against Ti6Al4V, CFRP stack and CFRP-Ti stacks in cross-cylinder configuration. The inset show cyclic variation in CoF while sliding against CFRP and Ti rings.

Fig. 7 show CoF variation of WC-Co cylinder sliding against different workpiece materials at sliding speed of 21.3 m/min and normal load of 20N. When sliding against Ti6Al4V cylinder, a sharp increase in the CoF appeared followed by steady CoF of 0.2. However, when the test was performed against the CFRP workpiece stack the friction increased initially followed by a short steady state CoF with a value of 0.15. With further increase in travel distance, the value of CoF against CFRP showed variable response. Whereas, sliding against CFRP-Ti stacks showed cyclic variation in the CoF. As the transition of the WC-Co cylinder take place from CFRP to Ti6Al4V ring during the test, a sharp increase in friction coefficient was observed. This could be due to the contact surface being freshly scrubbed against the fibrous composites oriented perpendicular to the tool cylinder. Thus, an active surface for interaction with the reactive titanium is readily

available that yields a higher adhesive response and an increased CoF. The inset of Fig. 7 show a shorter test on CFRP-Ti stacks to obtain more information about the transition of the tool cylinder from CFRP to titanium ring. It was found that a rapid increase in the CoF occurs at the interface of CFRP-Ti stack. In the literature, a similar increase in thrust force response was reported for drilling operation when the tool makes a transition from CFRP to titanium plate [31]. The variation in thrust forces could be attributed to the variation in the CoF/frictional forces experienced in the tribological contact between the tool and different workpiece constituents. As the frictional forces are higher against the titanium therefore, the thrust forces experienced while drilling of titanium would be higher. This excludes any effect of the machined chips and the influence of thickness of the titanium plate. The continuous cyclic variation of the frictional force would result in blunting of the tool edge quickly, considering a combination of adhesive and abrasive wear action contributing towards increased overall wear.

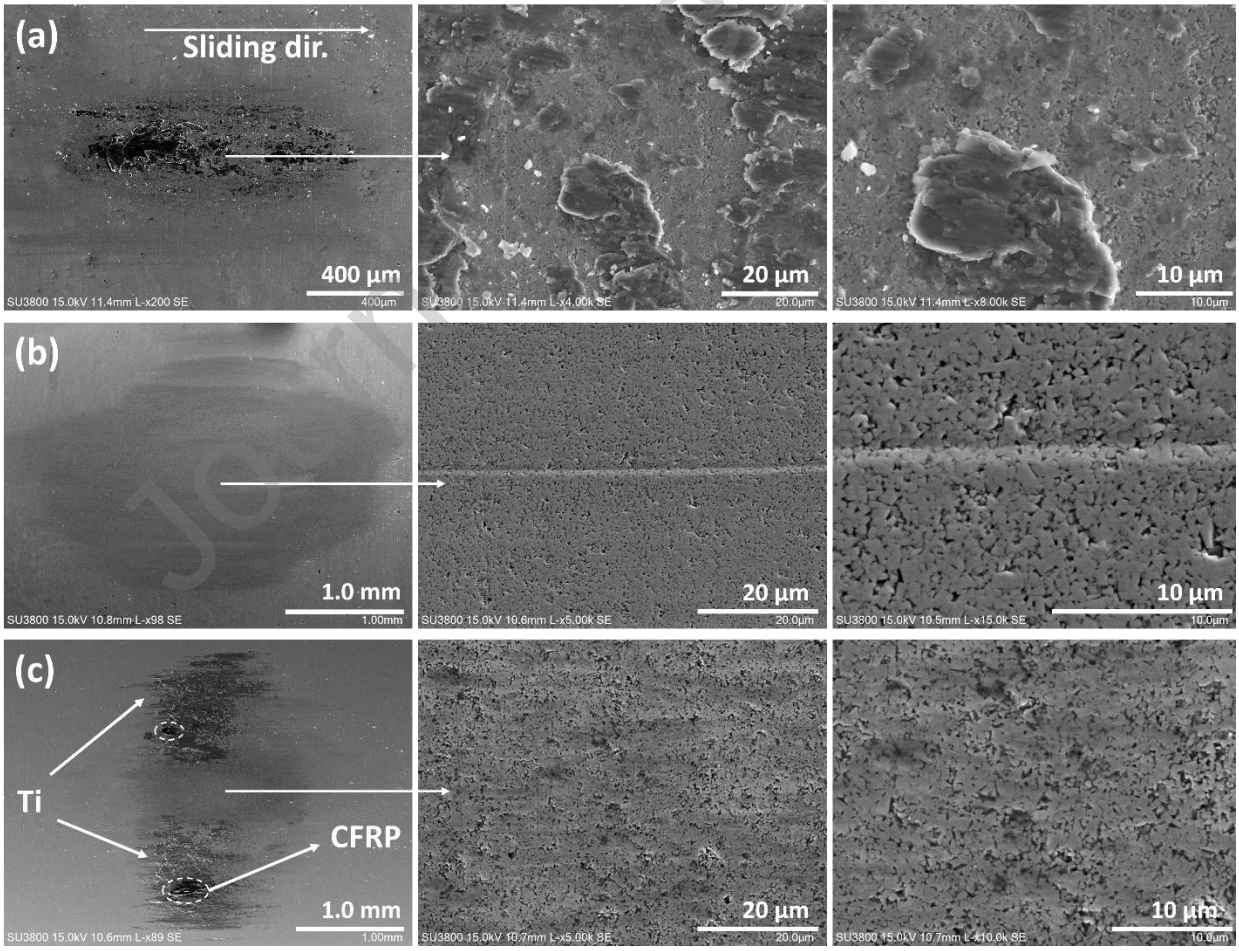

Fig. 8: Wear scars on WC-Co cylinder after sliding against a) Ti6Al4V b) CFRP and (c) CFRP-Ti stack.

Fig. 8 shows the SEM analysis of the WC-Co rods after sliding against Ti6Al4V, CFRP and CFRP-Ti stacks workpiece. As established earlier while sliding against Ti6Al4V tube, adhesive wear is predominant. However, while sliding against CFRP, abrasive marks were observed on the wear scar. The wear analysis of WC-Co cylinder sliding against CFRP-Ti stack showed a significantly higher amount of carbides grains dislodged in comparison to its sliding against CFRP. Moreover, across the periphery of the wear scar in test against CFRP-Ti workpiece, adhered titanium was observed. A closer examination in the middle of the wear scar showed localized adhesion of titanium on WC grains in CFRP-Ti case. The wear occurs progressively with twin action of adhesive and abrasive wear as evident from the wear scar in CFRP-Ti case. Therefore, one could confirm that higher wear was caused while sliding against CFRP-Ti stacks and the wear scar was quite complex revealing a synergistic aggressive action of the adhesion of titanium locally and in the periphery of the wear scar, with abrasive marks from CFRP and removal of WC grains.

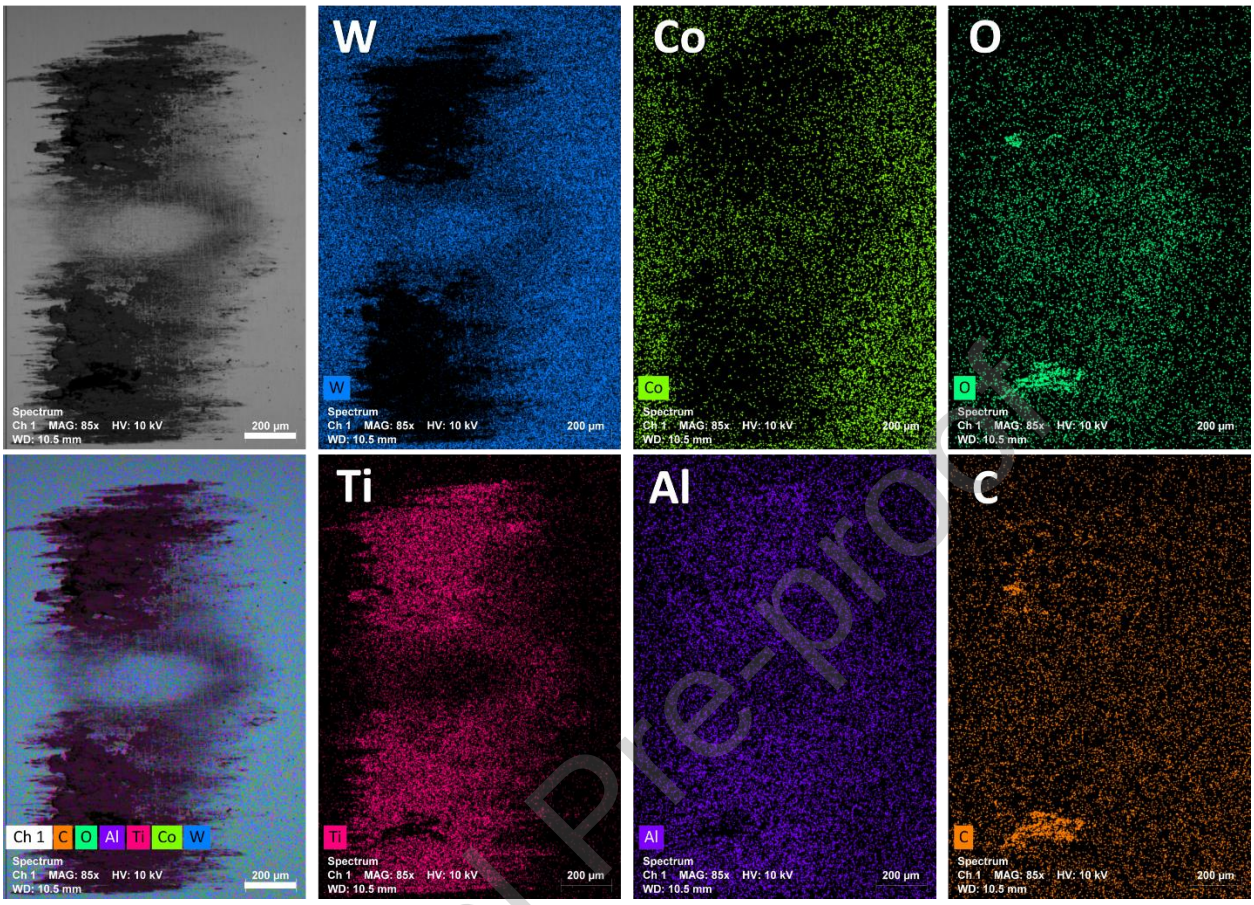

Fig. 9: EDX map of wear scar of the WC-Co cylinder after sliding against CFRP-Ti stack in cross-cylinder tribotest

Fig. 9 show the EDX map of the wear scar of WC-Co cylinder after sliding against multi-material stack of CFRP-Ti in cross-cylinder test configuration. The EDX map clearly shows the adhered titanium on the periphery of the wear scar with residue of carbon fiber across the wear scar. On a closer examination in middle of the wear scar adhered titanium in localized region was observed. This would be due to adhesive wear while sliding against Ti6Al4V ring, but when the tool cylinder makes a transition towards the CFRP ring, carbon fibers remove the adhered titanium and sometime can dislodge carbides grain adhered with transferred titanium. As known, tool wear in drilling of CFRP-Ti stacks occurs by high abrasive action of carbon fiber and adhesive action of reactive titanium [32,33]. The tool wear is aggravated causing dulling/chipping of edge and high flank wear occur that could lead to catastrophic failure.

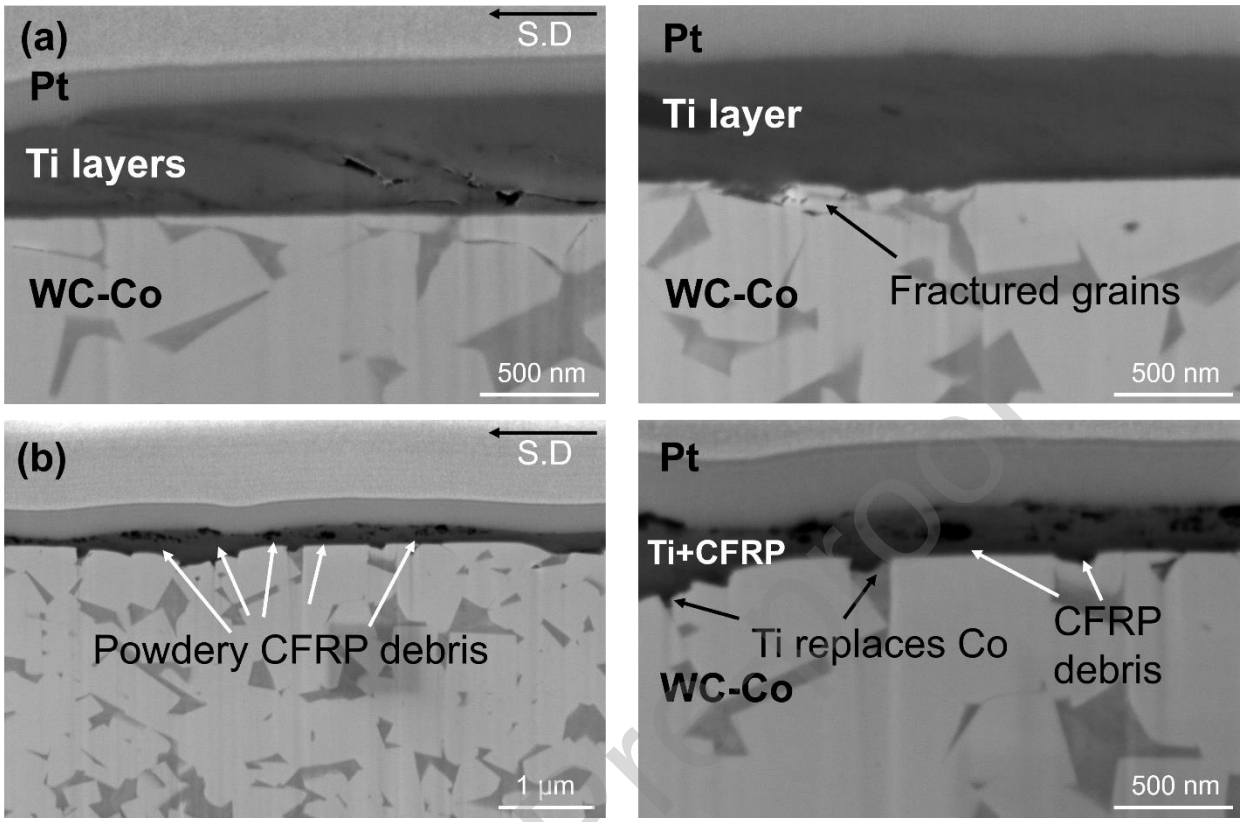

Fig. 10: FIB cross-section microscopy of WC-Co worn region tested against (a) Ti6Al4V workpiece at sliding speed of 71.3 m/min and (b) CFRP-Ti workpiece at sliding speed of 21.3 m/min. S.D stands for sliding direction.

Fig. 10a shows the SEM microscopy of the FIB cross-section of worn region of WC-Co cylinder tested against Ti6Al4V workpiece at 71.3m/min sliding speed. It shows the transferred titanium in the form of lumps on the contact region that is adhered layer by layer and present lamellar flow in the direction of sliding. It seems that during the testing, titanium is being adhered gradually over previously transferred titanium. The contact surface of WC appears smooth showing normal wear and region below few microns is affected predominantly by fracturing of the WC grains and their remotion. The transferred titanium also ingress and replace cobalt binder and small carbide fragments are intermixed with Ti. Whereas Fig. 10b shows cross-section of the worn region tested against CFRP-Ti stack, interestingly transferred titanium layer have black patches that would be CFRP powder debris produced while sliding against CFRP. The intermixing of titanium with CFRP powder debris would have occurred when WC slides across multiple titanium and CFRP rings in multi-material workpiece. In comparison, higher replacement of the Co binder and dislodged grains with transferred titanium was observed while sliding against CFRP-Ti stacks. The contact region also showed local depression that

corresponds to high wear, plastic deformation, and increased movement of WC grains. The removal of WC fragments and movement of WC grains could be due to brushing action of carbon fibers of composite. The abrasive fiber and powdery debris could easily reach in between the carbide grain and remove soft Co binder resulting in weakening of the substrate strength for easier evacuation of WC fragments and motion of the WC grains. Thus, in CFRP-Ti stacks machining, grain size distribution of WC grains and binding strength of the Co binder could significantly determine tool wear performance. Moreover, in correlation of FIB cross-section observation with tool wear in drilling of CFRP-Ti stacks, a similar 'powdery' composite chips formation is frequently reported that weld firmly with the cutting tool [5]. The embedded composite powder is highly abrasive in nature that causes roughening of the contact yielding in increased tool wear.

Thus, by using cross-cylinder configuration of tribotest, it is possible to mimic a similar wear mechanism response in a simple and controllable way. As can be seen that sliding against titanium showed adhesive wear while against CFRP showed abrasive wear. The wear against CFRP-Ti was aggravated response of abrasive and adhesive wear alongside occasional removal of cemented carbide grains forming smaller pits [34]. Further, in cross-cylinder test the workpiece shaft can be renewed repeatedly for continuation of the tribotest for a longer duration on the similar contact to emulate the wear mechanism for a long distance, while keeping a fresh countersurface.

Conclusions

- A cross-cylinder tribotest is an effective technique to emulate the wear mechanism during the drilling operation. For the first time, the new multi-material stack configuration in cross-cylinder tribotest was proposed for emulating the drilling operation of CFRP-Ti stacks. The wear mechanism during drilling of CFRP-Ti stack is a combination of adhesive and abrasive wear which was mimicked quite closely by a simple technique.
- While sliding against Ti6Al4V workpiece, adhesion dominates the wear mechanism. The adhesion increases with the increase in sliding speed which ultimately increases the CoF. On the other hand, CFRP workpiece showed abrasive wear response. A dual action of adhesive

and abrasive wear, which occurs for CFRP-Ti stacks, contributed towards an accelerated tool wear.

- Considering the simple acquisition process and ease of interchangeable workpiece material the testing methodology could easily be extended for other multi-material stacks combinations like CFRP-Al and CFRP-Al-GFRP etc.
- Cross-cylinder tribotest has great potential for a cost-effective and robust preliminary appraisal procedure for evaluating the performance of new coatings, prior to their use in drilling or machining operations.

Declaration of Interest

The authors declare that they have no known competing financial interests or personal relationships that could have appeared to influence the work reported in this paper.

Acknowledgement

This research was funded by European Union's Horizon 2020 research and innovation programme under the Marie Skłodowska-Curie grant agreement No. 860246. This research was sponsored by national funds through FCT – Fundação para a Ciência e a Tecnologia, under the project UIDB/00285/2020 and LA/P/0112/2020. The author would like to thank Dr. Marta Saraiva and Dr. Raphaël Royer at Sandvik Coromant, Sweden for valuable discussion, FIB analysis and providing the WC cylinders.

References

[1] Xu J, Mkaddem A, El Mansori M. Recent advances in drilling hybrid FRP/Ti composite: A state-of-the-art review. Compos Struct 2016;135:316–38. https://doi.org/10.1016/j.compstruct.2015.09.028.

[2] Xu J, Li C, Chen M, Ren F. A comparison between vibration assisted and conventional drilling of CFRP/Ti6Al4V stacks. Mater Manuf Process 2019;34:1182–93. https://doi.org/10.1080/10426914.2019.1615085.

[3] Xu J, Lin T, Li L, Ji M, Davim JP, Geier N, et al. Numerical study of interface damage formation mechanisms in machining CFRP/Ti6Al4V stacks under different cutting

sequence strategies. Compos Struct 2022;285:115236. https://doi.org/10.1016/j.compstruct.2022.115236.

[4] Xu J, Ji M, Chen M. On the quantitative analysis of drill edge wear when machining CFRP/Ti6Al4V stacks. Int J Adv Manuf Technol 2020;108:1463–72. https://doi.org/10.1007/s00170-020-05206-z.

[5] Xu J, Li C, Chen M, El Mansori M, Paulo Davim J. On the analysis of temperatures, surface morphologies and tool wear in drilling CFRP/Ti6Al4V stacks under different cutting sequence strategies. Compos Struct 2020;234:111708. https://doi.org/10.1016/j.compstruct.2019.111708.

[6] Nguyen D, Voznyuk V, Bin Abdullah MS, Kim D, Kwon PY. Tool Wear of Superhard Ceramic Coated Tools in Drilling of CFRP/Ti Stacks. Vol. 2 Process. Mater., vol. 2, American Society of Mechanical Engineers; 2019, p. 1–10. https://doi.org/10.1115/MSEC2019-2843.

[7] Wang X, Kwon PY, Sturtevant C, Kim D (Dae-W, Lantrip J. Comparative tool wear study based on drilling experiments on CFRp/Ti stack and its individual layers. Wear 2014;317:265–76. https://doi.org/10.1016/j.wear.2014.05.007.

[8] Xu J, Chen M, Paulo Davim J, El Mansori M. A Review on the Machinability of Aerospace-Grade CFRP/Titanium Stacks. Adv Mater Lett 2021;12:1–7. https://doi.org/10.5185/amlett.2021.011591.

[9] Xu J, El Mansori M. Wear characteristics of polycrystalline diamond tools in orthogonal cutting of CFRP/Ti stacks. Wear 2017;376–377:91–106. https://doi.org/10.1016/j.wear.2016.11.038.

[10] Xu J, El Mansori M, Chen M, Ren F. Orthogonal cutting mechanisms of CFRP/Ti6Al4V stacks. Int J Adv Manuf Technol 2019;103:3831–51. https://doi.org/10.1007/s00170-019-03734-x.

[11] Xu J, El Mansori M, Voisin J, Chen M, Ren F. On the interpretation of drilling CFRP/Ti6Al4V stacks using the orthogonal cutting method: Chip removal mode and subsurface damage formation. J Manuf Process 2019;44:435–47.

https://doi.org/10.1016/j.jmapro.2019.05.052.

[12] Park KH, Beal A, Kim DDW, Kwon P, Lantrip J. Tool wear in drilling of composite/titanium stacks using carbide and polycrystalline diamond tools. Wear 2011;271:2826–35. https://doi.org/10.1016/j.wear.2011.05.038.

[13] Zhu B, Mardel J, Kelly GL. An Investigation of Tribological Properties of CN and TiCN Coatings. J Mater Eng Perform 2004;13:481–7. https://doi.org/10.1361/10599490420025.

[14] Gerth J, Heinrichs J, Nyberg H, Larsson M, Wiklund U. Evaluation of an intermittent sliding test for reproducing work material transfer in milling operations. Tribol Int 2012;52:153–60. https://doi.org/10.1016/j.triboint.2012.03.015.

[15] Olander P, Heinrichs J. Initiation and propagation of tool wear in turning of titanium alloys – Evaluated in successive sliding wear test. Wear 2019;426–427:1658–66. https://doi.org/10.1016/j.wear.2019.01.077.

[16] Hedenqvist P, Olsson M, Söderberg S. Influence of Tin Coating on Wear of High Speed Steel Tools as Studied by New Laboratory Wear Test. Surf Eng 1989;5:141–50. https://doi.org/10.1179/sur.1989.5.2.141.

[17] Sato T, Tada Y, Ozaki M, Hoke K, Besshi T. A crossed-cylinders testing for evaluation of wear and tribological properties of coated tools. Wear 1994;178:95–100. https://doi.org/10.1016/0043-1648(94)90133-3.

[18] Ramalho A. Micro-Scale Abrasive Wear Test of Thin Coated Cylindrical Surfaces. Tribol Lett 2004;16:133–41. https://doi.org/10.1023/B:TRIL.0000009723.03977.47.

[19] Heinrichs J, Gerth J, Bexell U, Larsson M, Wiklund U. Influence from surface roughness on steel transfer to PVD tool coatings in continuous and intermittent sliding contacts. Tribol Int 2012;56:9–18. https://doi.org/10.1016/j.triboint.2012.06.013.

[20] Heinrichs J, Gerth J, Thersleff T, Bexell U, Larsson M, Wiklund U. Influence of sliding speed on modes of material transfer as steel slides against PVD tool coatings. Tribol Int 2013;58:55–64. https://doi.org/10.1016/j.triboint.2012.09.012.

[21] Aiso T, Wiklund U. Influence of contact parameters on material transfer from steel to TiN

coated tool – optimisation of a sliding test for simulation of material transfer in milling. Tribol - Mater Surfaces Interfaces 2016;10:107–16. https://doi.org/10.1080/17515831.2016.1202548.

[22] Aiso T, Wiklund U, Kubota M, Jacobson S. Effect of Si and Cr additions to carbon steel on material transfer in a steel/TiN coated tool sliding contact. Tribol Int 2016;97:337–48. https://doi.org/10.1016/j.triboint.2016.01.032.

[23] Aiso T, Wiklund U, Kubota M, Jacobson S. Influence of Mn and Al additions to carbon steel on material transfer and coating damage mechanism in a sliding contact between steel and TiN coated HSS tool. Tribol Int 2016;101:414–24. https://doi.org/10.1016/j.triboint.2016.04.036.

[24] Heinrichs J, Olsson M, Jacobson S. Initial deformation and wear of cemented carbides in rock drilling as examined by a sliding wear test. Int J Refract Met Hard Mater 2017;64:7–13. https://doi.org/10.1016/j.ijrmhm.2016.12.011.

[25] Vite-Torres M, Gallardo-Hernández EA, Cruz-Ovando E. Experimental study of adhesive wear of a holding device using a cross cylinders tester. Tribol Ind 2015;37:354–9.

[26] Heinrichs J, Norgren S, Jacobson S, Yvell K, Olsson M. Influence of binder metal on wear initiation of cemented carbides in sliding contact with granite. Wear 2021;470–471:203645. https://doi.org/10.1016/j.wear.2021.203645.

[27] Mikado H, Heinrichs J, Wiklund U, Jacobson S. Wear of uncoated and PVD coated cemented carbide tools for processing of copper based materials part I: Lab test verification in dry and lubricated sliding. Wear 2020;462–463:203487. https://doi.org/10.1016/j.wear.2020.203487.

[28] Heinrichs J, Mikado H, Wiklund U, Jacobson S. Wear of uncoated and PVD coated cemented carbide tools for processing of copper based materials part II: Exploring the sliding contact with pure copper. Wear 2021;466–467:203589. https://doi.org/10.1016/j.wear.2020.203589.

[29] Fan Y, Hao Z, Zheng M, Yang S. Wear characteristics of cemented carbide tool in dry-machining Ti-6Al-4V. Mach Sci Technol 2016;20:249–61.

https://doi.org/10.1080/10910344.2016.1165837.

[30] Yuan CG, Pramanik A, Basak AK, Prakash C, Shankar S. Drilling of titanium alloy (Ti6Al4V) – a review. Mach Sci Technol 2021;25:637–702. https://doi.org/10.1080/10910344.2021.1925295.

[31] Qi Z, Ge E, Yang J, Li F, Jin S. Influence mechanism of multi-factor on the diameter of the stepped hole in the drilling of CFRP/Ti stacks. Int J Adv Manuf Technol 2021;113:923–33. https://doi.org/10.1007/s00170-021-06678-3.

[32] Geier N, Davim JP, Szalay T. Advanced cutting tools and technologies for drilling carbon fibre reinforced polymer (CFRP) composites: A review. Compos Part A Appl Sci Manuf 2019;125:105552. https://doi.org/10.1016/j.compositesa.2019.105552.

[33] Xu J, Ji M, Paulo Davim J, Chen M, El Mansori M, Krishnaraj V. Comparative study of minimum quantity lubrication and dry drilling of CFRP/titanium stacks using TiAlN and diamond coated drills. Compos Struct 2020;234:111727. https://doi.org/10.1016/j.compstruct.2019.111727.

[34] Li S, Qin X, Jin Y, Sun D, Li Y. A comparative study of hole-making performance by coated and uncoated WC/Co cutters in helical milling of Ti/CFRP stacks. Int J Adv Manuf Technol 2018;94:2645–58. https://doi.org/10.1007/s00170-017-0842-8.

Declaration of interests

☒The authors declare that they have no known competing financial interests or personal relationships that could have appeared to influence the work reported in this paper.

☐The authors declare the following financial interests/personal relationships which may be considered as potential competing interests:

Highlights:

- *Enhancement and construction of cross-cylinder test for novel stack materials*
- *Exploitation of cross-cylinder tribotest for wear analysis of tool sliding against multi-material stack of CFRP-Ti rings*
- *Wear mechanism analysis of WC-Co tool sliding against Ti6Al4V alloy, CFRP stacks and CFRP-Ti stacks*
- *Simple tribotest configuration for emulating contact situation similar to drilling operation.*

Statement of Originality

As the corresponding author, I certify that this manuscript is original and its publication doesnot infringe any copyrights.

As the corresponding author I declare that the manuscript has not been previously published, in whole or in part in any other journal or scientific publishing company. Also, the manuscript does not participate in any other publishing process. I also declare there is no conflict of interest.

As the corresponding author I declare that all persons listed hereafter were committed in the creation of the paper and were informed about their participation.